Électrotechnique et électroénergétique

INCLINATION SENSING CAPABILITIES OF A SYMMETRICAL PERMANENT MAGNET LEVITATION SETUP WITH ELECTROMAGNETS AND DIAMAGNETIC STABILIZATION

IOSIF VASILE NEMOIANU, VERONICA MANESCU (PALTANEA), GHEORGHE PALTANEA

Sensing capabilities as tiltmeter presented by a setup realized with two identical coaxial cylindrical coils, in which a small permanent magnet is levitated in between, are investigated. As stabilizing pieces two pyrolitic graphite sheets are used, not to contradict Earshaw's theorem which prohibits all kind of stable levitation in fields having a magnitude inversely proportional to the squared distance. The flux density associated to the coils is analytically evaluated, to be further used to derive the magnetic force needed to balance the force of gravity when levitation occurs. The used approximation is that the helical conductor presented by a coil is assumed to be an arrangement of aligned tangent circular loops. Equilibrium point coordinates of the levitated magnet are evaluated for tilt angles varying from horizontal to vertical positions. Conversion characteristics, stability functions and sensitivities for this possible kind of tiltmeter are obtained and discussed.

1. INTRODUCTION

Passive levitation occurring in time-invariant magnetic fields (either produced by permanent magnets or by dc supplied electromagnets) presents essentially two main aspects [1].

First, levitation of a permanent magnet embedded in such a field always requires the presence of a diamagnetic material in its close proximity to stabilize equilibrium. Indeed, Earnshaw's theorem states that no stable equilibrium is achievable within a system of bodies interacting through fields inversely proportional to distance squared magnitudes. The introduced diamagnetic body provides the permanent magnet with the adaptive restoring forces necessary to counteract any small displacement around the equilibrium point achieving thus stability. Variants with multiple simultaneously levitated permanent magnets are also possible in association with stabilizing diamagnetic pieces, too. In this case, the magnetostatics problem of finding each magnets' equilibrium point is more complex since the levitated bodies are mutually interacting one with the other [2].

Second kind of levitation is the levitation of diamagnetic bodies themselves. Inherently stable, the suspension occurs when the force of gravity is balanced by the diamagnetic forces developed by the inhomogeneity of the magnetic field in which the suspended body is introduced. That is to say that diamagnetic bodies are repelled from the regions where the magnetic field is more intense. Although weak the diamagnetic force may balance gravity in the case of small bodies [3–5].

Levitation structures address a large array of technical applications, to mention sensing (tiltmeters, seismometers), micro-electromechanical systems (MEMS), magnetic bearings, micromotors, but even energy harvesting devices etc. [6–11].

The levitator under scrutiny [12], belonging to the first enumerated category, presents several sensing applications, among which we are focusing in this paper on inclination sensing capabilities, only. The paper is organized as follows:

- Section 2 is dedicated to problem description (geometry, materials, balance of forces, equilibrium and stability).
- Section 3 presents the analytical model used to compute the magnetic force acting on the levitated magnet.
- Section 4 is dedicated to simulating the performance of a possible tiltmeter based on the proposed levitation structure (conversion characteristics, stability functions, sensitivities).
- Section 5 is dedicated to conclusions and discussing the obtained results.

2. PROBLEM DESCRIPTION

2.1. INCLINED SYMMETRICAL COAXIAL DC COIL LEVITATION SYSTEM OF A SMALL PERMANENT MAGNET USING STABILIZING DIAMAGNETIC SHEETS.

Levitator's global structure is depicted in Fig. 1. Two identical coaxial cylindrical coils (I and II) are aligned to the z-axis of a Cartesian system of coordinates, whose center is at mid distance from the right and left ends of Coil I and Coil II, respectively. Distance D is measured from the left and right ends of the same respective solenoids. The coils are dc supplied with the same current of intensity I_0. The inner and outer radii of the coils, r_1 and r_2, are considered with respect to the wire conductor centers. For simplicity reasons, aiming to further allow a more convenient analytical computation of the flux density, a matrix arrangement of the winding conductor is considered. Zone A from Fig. 1 is zoomed in, as shown in Fig. 2, where the assumed approximation is more visible. There are N_z rows and N_x columns of the circular section wires, all tangent to each other, constituting the windings' model. The coils' length is L, also measured from the axis of the left and right columns conductors.
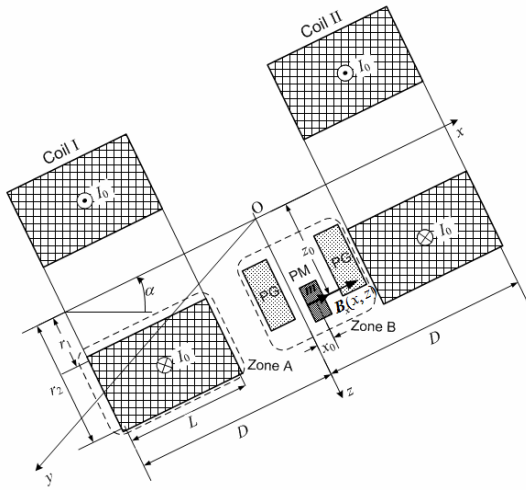
"Politehnica" University of Bucharest, E-mail: [iosif.nemoianu, veronica.paltanea, gheorghe.paltanea]@upb.ro.

Fig. 1 – Inclined passive levitation structure of a small permanent magnet (PM) (Tilt angle is α.) Two identical coaxial cylindrical coils (I and II), in which runs a dc current, produce the magnetic field in which levitation state is achieved. Stabilization at the equilibrium point is ensured by two pyrolitic graphite sheets (PG) placed perpendicular to the coils' axis. The origin of the Cartesian frame of reference origin (O) lies at mid distance on the axis of the coils.
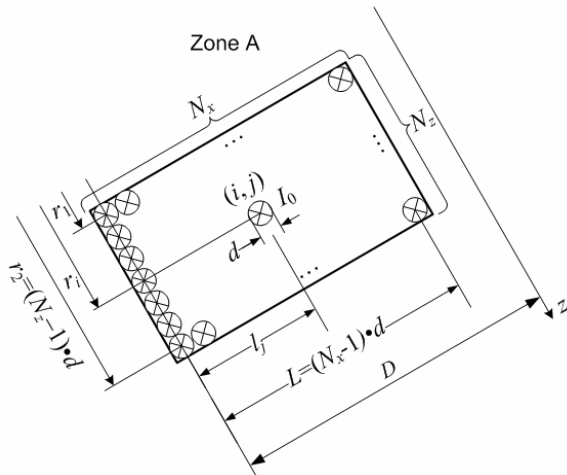

Fig. 2 – Detailed view on zone A, shown in Fig. 1 of a cross section of Coil I winding (the same as for Coil II). Position of the turns within the winding is idealized to a matrix disposition with N_z rows and N_x columns, circumscribed to a rectangle.

Returning to Fig. 1, it can be noticed the small Nd-Fe-B permanent magnet (PM) which levitates as a result of the magnetic forces developed by the coils, at the point they cancel out the force of gravity, *i.e.* (x_0, y_0). According to Earnshaws's theorem one or two diamagnetic plates made of pyrolitic graphite (PG) are necessary to stabilize levitation. When tilting the whole structure with angle α, it can be assumed that the mounting part of the PG plates is allowed to move freely with the levitated PM to achieve equilibrium. A more detailed view of zone B is provided in Fig. 3, showing the disc PM radius R, its thickness l and the equal separation s from the two PG sheets. Another approximation, also used in [13], assumes that the PM disc is parallel to the PG plates and all with the yz-plane. In both Figs. 1 and 3, $\boldsymbol{m}$ denotes the magnetic moment vector of the PM and $\boldsymbol{B}_x(x, y)$ the flux density x-vector component, the sole to develop magnetic forces along the x- and z- axes, as it will be proven in Section 2. As a result of the assumption made, the magnetic moment $\boldsymbol{m}$ is also parallel to the x-axis.

It can be also proven that any of the PG plates can be removed, case in which the equilibrium point slightly shifts toward the remaining plate. Thus, single plate structures are also possible.
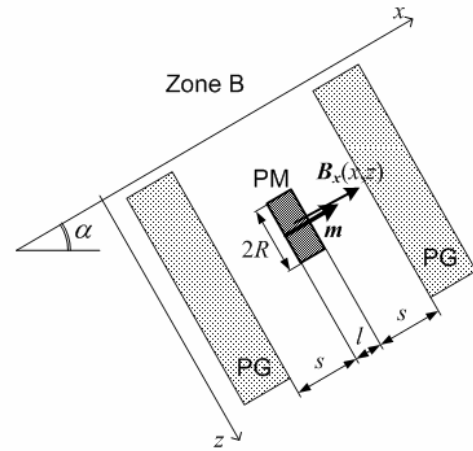

Fig. 3 – Detailed view on zone B, shown in Fig. 1. Two pyrolitic graphite sheets stabilize PM's levitation along x-axis. Equal separation from the PG sheets s is considered on each side of the PM of radius R and thickness l. The PM's magnetic moment is $\boldsymbol{m}$ and $\boldsymbol{B}_x(x, z)$ the local vector of flux density x-component of the magnetic field associated to the coils.

2.2. BALANCE OF FORCES. EQUILIBRIUM STABILITY

As mentioned in the previous Subsection 2.1., the force $\boldsymbol{F}_m$ developed in the time-invariant magnetic field produced by the coils must balance the PM force of gravity $\boldsymbol{G}$ in order to achieve levitation, as shown in Fig. 4. In accordance with Earnshaw's theorem, an elementary displacement around the equilibrium point must be compensated by an adaptive external force, namely the diamagnetic forces generated by the presence of the PG plates. If two symmetrically placed plates are considered, the diamagnetic forces have no influence in establishing the equilibrium point position. Indeed, these forces have equal magnitude, but act in opposite directions. Therefore, they cancel each other out. For the sake of simplicity, in Fig. 4 the PG plates are not considered, neither are the corresponding diamagnetic forces that would act on the floating PM.

A possible global approach may start from the total potential energy possessed by the PM in gravitational and magnetic fields combined [14]:

$$U(x, y, z) = -\boldsymbol{m} \cdot \boldsymbol{B}(x, y, z) - G\, h(x, z), \qquad (1)$$

where the force of gravity $G = \gamma V g$, γ is the mass density of the material, $V = \pi R^2 l$ is its volume and g is the gravitational acceleration magnitude. Elementary geometric and trigonometric calculations provide the height as function of x and z coordinates $h(x, z) = z \cos\alpha - x \sin\alpha$ corresponding to the center of mass with respect to an arbitrary reference, *e.g.* the origin of the reference frame, as shown for the equilibrium point in Fig. 4.

Therefore, with (1), we get [14]

$$U(x, 0, z) = -m\, B_x(x, 0, z) - G\, (z \cos\alpha - x \sin\alpha). \ (2)$$

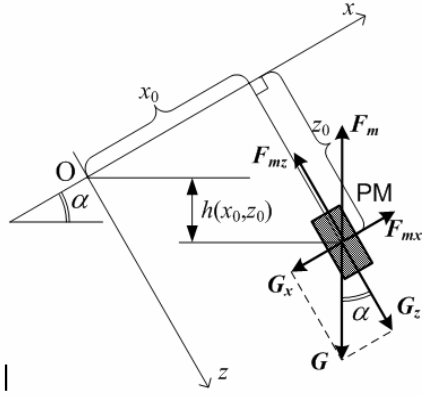By taking the negative gradient of U, given by (2), the total force acting on the PM becomes

Fig. 4 – Balance of forces acting on the PM at point (x_0, z_0). The force of gravity G is balanced by the magnetic force F_m, all being considered at the PM's center of mass which height at the equilibrium point $h(x_0, z_0)$ is referenced from the origin of the system of coordinates. Pyrolitic graphite plates (PG) are not shown.

$$F_{total} = -\nabla U = \underbrace{\left(m\frac{\partial B_x}{\partial x}\bigg|_{y=0}\right)}_{F_{mx}} i + \underbrace{\left(m\frac{\partial B_x}{\partial z}\bigg|_{y=0}\right)}_{F_{mz}} k - \underbrace{(G\sin\alpha)i}_{G_x} + \underbrace{(G\cos\alpha)k}_{G_z}, \quad (3)$$

where i and k are the x- and z-axes unit vectors, respectively. On components, from (3), the condition $F_{total} = 0$ produces a system of equations [14]

$$\begin{cases} m\dfrac{\partial B_x}{\partial z}\bigg|_{y=0} + G\cos\alpha = 0 \\[2mm] m\dfrac{\partial B_x}{\partial x}\bigg|_{y=0} - G\sin\alpha = 0. \end{cases} \quad (4)$$

Note that, by symmetry reasons, the equilibrium point is expected to belong to the xz- plane (for $y = 0$). For $\alpha = 0$, it is obvious that $x_0 = 0$ and z_0 is only obtained by solving the equation

$$m\frac{\partial B_x}{\partial z}\bigg|_{\substack{x=0 \\ y=0}} + G = 0. \quad (5)$$

Conversely, if $\alpha = \pi/2$ is expected that $z_0 = 0$ and x_0 to be the solution of

$$m\frac{\partial B_x}{\partial x}\bigg|_{\substack{y=0 \\ z=0}} - G = 0. \quad (6)$$

In order to be stable, the following quantities termed stability functions (discriminants) must be simultaneously positive [2, 12, 14]:

$$D_x = \frac{\partial^2 U}{\partial x^2}\bigg|_{\substack{x=x_0 \\ y=0 \\ z=z_0}} > 0, \quad D_y = \frac{\partial^2 U}{\partial y^2}\bigg|_{\substack{x=x_0 \\ y=0 \\ z=z_0}} > 0$$

and

$$D_z = \frac{\partial^2 U}{\partial z^2}\bigg|_{\substack{x=x_0 \\ y=0 \\ z=z_0}} > 0. \quad (7)$$

With (1), this reduces (up to a factor) to similar conditions imposed on the second derivative of B_x, namely [2, 12, 14]

$$D_x = -m\frac{\partial^2 B_x}{\partial x^2}\bigg|_{\substack{x=x_0 \\ y=0 \\ z=z_0}} > 0, \quad D_y = -m\frac{\partial^2 B_x}{\partial y^2}\bigg|_{\substack{x=x_0 \\ y=0 \\ z=z_0}} > 0$$

and

$$D_z = -m\frac{\partial^2 B_x}{\partial z^2}\bigg|_{\substack{x=x_0 \\ y=0 \\ z=z_0}} > 0. \quad (8)$$

The negative value of a stability function, evaluated at the equilibrium point, will indicate, according to Earnshaw's theorem, the necessity of introducing stabilization piece(s) along the respective axis direction (one or two PG sheets perpendicular to the axis along which stabilization is needed). The introduction of two stabilizing PG sheets leads to the addition of the following term to the stability function (value taken at the equilibrium point) [2, 12, 14], called the diamagnetic influence factor:

$$C = \frac{\mu_0 m^2 |\chi|}{16\pi(s+R)^5}, \quad (9)$$

where $|\chi|$ is the magnetic susceptibility absolute value of pyrolitic graphite (one of the greatest achievable values at room temperature along a direction perpendicular to the sheets) and μ_0 is the vacuum permeability (see Fig. 3). Note that, according to [15], for (9) to be valid, the distances s, l and the thickness of the PG sheets are such that the PM's images are fully contained within the sheets volume.

Magnetic moment of the levitated PM is given in [14] as

$$m = B_r V / \mu_0, \quad (10)$$

where B_r is the remanence of the PM Nd-Fe-B material.

3. ANALYTICAL MODEL FOR FORCE AND STABILITY FUNCTIONS COMPUTATION

As it was first suggested in Fig. 2, a matrix of circular section wires will be considered [12]. Generally, obtaining an analytical formula for the B-fields in the case of a coil is not an easy undertaking, being mostly carried out numerically [16, 17]. In our approach, the aforementioned approximation will provide an analytical formula for the flux density, allowing thus to perform the derivatives appearing in (4), (5), (6) and (8).

The flux density component B_x has two terms each corresponding to one of the coils, namely

$$B_x(x,z) = B_{I,x}(x,z) + B_{II,x}(x,z). \quad (11)$$

Moreover, each term from (10) is the superposition of the effects of the corresponding circular loops of indices (i, j) belonging to each coil matrix (I or II) [12], as depicted in Fig. 2.

$$B_{I,x}(x,z) = \sum_{i=1}^{N_z}\sum_{j=1}^{N_x} B_{I,x,ij}(x,z),$$
$$B_{II,x}(x,z) = \sum_{i=1}^{N_z}\sum_{j=1}^{N_x} B_{II,x,ij}(x,z), \quad (12)$$

where

$$B_{\text{I},x,ij}(x,z) = \frac{\mu_0 I_0}{2\pi\sqrt{(r_i+z)^2+(x+D-l_j)^2}} \times$$
$$\times[\text{K}(k_{\text{I},ij}) + A_{\text{I},ij}\,\text{E}(k_{\text{I},ij})];$$

$$A_{\text{I},ij} = \frac{r_i^2 - z^2 - (x+D-l_j)^2}{(r_i-z)^2 + (x+D-l_j)^2};$$

$$k_{\text{I},ij} = 2\sqrt{\frac{r_i\,z}{(r_i+z)^2+(x+D-l_j)^2}};$$

$$B_{\text{II},x,ij}(x,z) = \frac{\mu_0 I_0}{2\pi\sqrt{(r_i+z)^2+(x+D-l_j)^2}} \times$$
$$\times[\text{K}(k_{\text{II},ij}) + A_{\text{II},ij}\,\text{E}(k_{\text{II},ij})]\ ;$$

$$A_{\text{II},ij} = \frac{r_i^2 - z^2 - (x-D+L-l_j)^2}{(r_i-z)^2 + (x-D+L-l_j)^2};$$

$$k_{\text{II},ij} = 2\sqrt{\frac{r_i\,z}{(r_i+z)^2+(x-D+L-l_j)^2}},\quad \text{with}$$

$$r_i = r_1 + (i-1)d,\ l_j = (j-1)d,\ i = 1,...,N_z, \qquad (13)$$
$$j = 1,...,N_x \qquad \text{and} \qquad L = (N_x-1)d.$$

In (13), K and E are the complete elliptic integrals of the first and second kind, respectively, and all the appearing geometrical parameters are shown in Fig. 2.

All the partial derivatives from (4), (5), (6) and (8) can be now obtained analytically with (11), (12) and (13).

4. SIMULATION RESULTS

In order to assess the possible use of the device shown in Fig. 1 as a tiltmeter, a numerical illustrative simulation is proposed. Simulation parameters are organized in Table 1.

Table 1

Parameters used for simulation

Parameter	Value
Intensity of the current supplying the coils	$I_0 = 9$ A
Number of conductors along x-axis (number of turns per layer)	$N_x = 12$
Number of conductors along z-axis (number of coil layers)	$N_z = 10$
Conductor diameter (standardized value)	$d = 1.29$ mm
Coils' inner radius	$r_1 = 50$ mm
Coils' outer radius [a]	$r_2 = 61.61$ mm
Coils' length [a]	$L = 14.19$ mm
Distance D (see Figs. 1 and 2)	$D = 50$ mm
Levitated PM radius	$R = 2.5$ mm
Levitated PM thickness	$l = 1$ mm
Remanence of the PM material (grade N45) [b]	$B_r = 1.3$ T
PM magnetic moment magnitude [c]	$m = 0.0203$ A·m^2
Mass density of Nd-Fe-B used for the PM	$\gamma = 7923$ kg/m^3
Separation between PM and PG plates	$s = 1.5$ mm
PG perpendicular susceptibility value	$\chi = -45\cdot10^{-5}$

[a] There values are not independent; they result from d and N_z or N_x.
[b] Remanence is slightly diminished to take into account self-demagnetization of the cylindrical PM in open-loop, as considered in [2, 14].
[c] This value is not independent; it results from R, l and B_r.

Solution of the system of nonlinear equations (4) is obtained using a general-purpose mathematics package, comprising a symbolic calculation module capable to carry out the first and second derivatives computation necessary in (4), (5), (6) and (8). Next, the system of equations (4) or equations (5) and (6), for the particular values $\alpha = 0$ and $\alpha = \pi/2$, respectively, are solved numerically. An angular displacement in equal steps of 5° between these two limits (horizontal and vertical positions) gives the equilibrium point coordinates shown in Table 2. ($y_0 = 0$ as a result of the symmetry of the device with respect to xz-plane in which levitation occurs).

Table 2

Simulation results for angular displacement

Tilt angle [degrees]	x_0 [mm]	z_0 [mm]
0	0.00	19.91
5	0.74	19.87
10	1.48	19.74
15	2.22	19.53
20	2.96	19.23
25	3.71	18.85
30	4.46	18.37
35	5.21	17.81
40	5.98	17.15
45	6.76	16.40
50	7.56	15.54
55	8.37	14.56
60	9.22	13.45
65	10.10	12.18
70	11.03	10.71
75	12.02	8.97
80	13.07	6.82
85	14.14	3.98
90	14.75	0.00

For a more convenient interpretation of the data contained in Table 2, a plot of the two equilibrium point coordinates is shown in Fig. 5.

Validity of the obtained result can be assessed by calculating the stability function values corresponding to the equilibrium points coordinates, as shown in Table 3, and plotted in Fig. 6.

Table 3

Simulation results for stability functions along the three axes

Tilt angle (degrees)	D_x [J/m^2]	D_y [J/m^2]	D_z [J/m^2]	D_x+C [J/m^2]
0	− 0.180	0.077	0.104	0.255
5	− 0.180	0.077	0.104	0.255
10	− 0.179	0.076	0.103	0.256
15	− 0.177	0.075	0.102	0.258
20	− 0.175	0.075	0.101	0.260
25	− 0.172	0.073	0.100	0.263
30	− 0.168	0.072	0.098	0.267
35	− 0.164	0.070	0.096	0.271
40	− 0.158	0.068	0.094	0.277
45	− 0.152	0.066	0.091	0.283
50	− 0.145	0.063	0.088	0.290
55	− 0.137	0.060	0.085	0.299
60	− 0.127	0.057	0.082	0.308
65	− 0.117	0.053	0.079	0.318

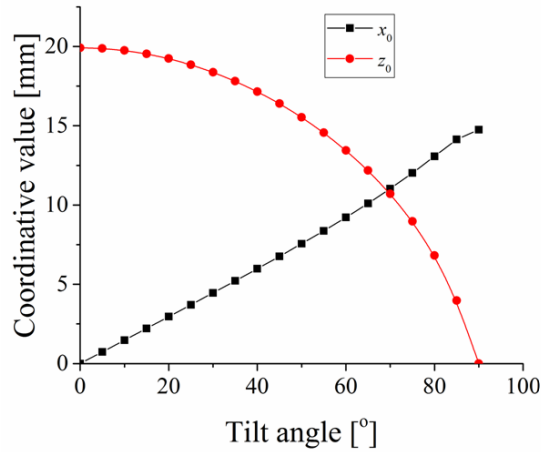|				(continuated)
70	− 0.106	0.049	0.075	0.329
75	− 0.094	0.044	0.071	0.341
80	− 0.081	0.039	0.068	0.354
85	− 0.068	0.033	0.064	0.367
90	− 0.061	0.030	0.063	0.375

Fig. 5 – Equilibrium point coordinates x_0 and z_0 vs. tilt angle (interpolated plots).
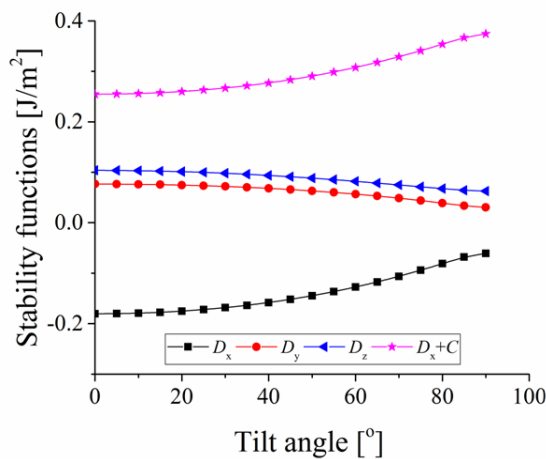

Fig. 6 – Stability functions at equilibrium point coordinates x_0 and z_0 vs. tilt angle (interpolated plots).
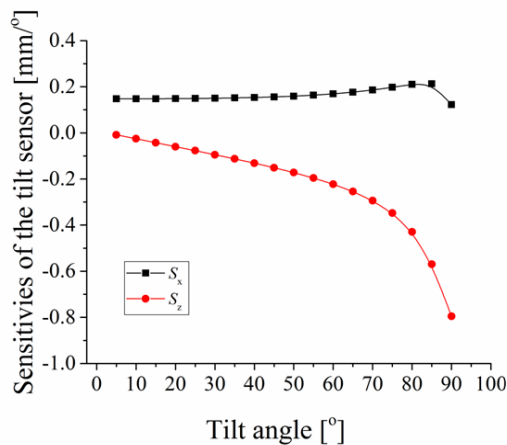

Fig. 7 – Sensitivities S_x and S_z vs. tilt angle (interpolated plots).

As expected, the negative values of D_x obtained for all tilt angles shown in Table 3, prove the necessity of introducing stabilizing PG sheets. With (9) and the corresponding values taken from Table 1, we get the diamagnetic influence factor $C = 0.435$ J/m^2. The last column in Table 3 corresponds to the sum $D_x + C > 0$, showing that stable levitation has been achieved in all cases.

An estimation of the feasibility for using this type of levitator as a tiltmeter is provided by the sensitivities presented by the sensor, regarded as a single input (the tilt angle α), but a two output device x_0 and z_0:

$$S_x = \frac{\mathrm{d}\,x_0}{\mathrm{d}\,\alpha} \text{ and } S_z = \frac{\mathrm{d}\,z_0}{\mathrm{d}\,\alpha}. \tag{14}$$

The two sensitivities plots are shown in Fig. 7.

5. CONCLUSIONS

A possible tiltmeter based on the presented levitator can operate in a non-magnetic environment. (All ferromagnetic pieces and other permanent magnets are sufficiently distant from the levitator.) Validity of the adopted model resides in two initially expected particular results. Firstly, for the horizontal position ($\alpha = 0$) $x_0 = 0$ and for the vertical one ($\alpha = \pi/2$) $z_0 = 0$. Secondly, in all the cases the stability function value D_x resulted negative, proving thus the necessity of introducing at least one stabilizing PG sheet as shown in Table 3 or Fig. 6. This behavior was also expected from the very beginning of the study.

An important characteristic of a tiltmeter operating on the principle of the proposed levitator is redundancy, which is beneficial in any measurement device. Information can therefore be extracted from two output conversion characteristics, for example, those shown in Fig. 5. Interestingly, the two conversion characteristics present significantly different sensitivities for the two output values x_0 and z_0. By examining the graph of x_0 shown in Fig. 5, it turns out that it is quite linear (up to about 85° tilt angle), fact reflected in an approximately constant sensitivity S_x (about 0.16 mm/deg.), as one can notice in Fig. 7. Unfortunately, the displacement with tilt angle is less pronounced along x-axis as it is for the z-axis, for which sensitivity S_z has a less convenient variation.

Other possible directions for using the presented levitator in sensing may be found for the horizontal variant ($\alpha = 0$). First, as a linear displacement sensor, when z_0 is function of the distance between the coils (variation of distance parameter D). Second, as a current intensity measuring device, when z_0 is function of the current carried by the coils (variation of parameter I_0).

REFERENCES

1. G. Küstler, *Diamagnetic levitation, Historical milestones*, Rev. Roum. Sci. Techn.–Électrotechn. et Énerg., **52**, *3*, pp. 265–282 (2007).
2. G. Küstler, I.V. Nemoianu, E. Cazacu, *Theoretical and experimental investigation of multiple horizontal diamagnetically stabilized levitation with permanent magnets*, IEEE Trans. Mag., **48**, *12*, pp. 4793–4801 (2012).
3. M.D. Simon, A.K. Geim, *Diamagnetic levitation: Flying frogs and floating magnets* (invited), J. Appl. Phys., **87**, *9*, pp. 6200–6204 (2000).
4. E. Cazacu, I.V. Nemoianu, *Estimation of the influence terms involved in static diamagnetic levitation*, Rev. Roum. Sci. Techn.–Électrotechn. et Énerg., **52**, *3*, pp. 283–290 (2007).
5. E. Cazacu, I.V. Nemoianu, *Diamagnetic levitation setting with enlargement of the stability area*, Rev. Roum. Sci. Techn.–Électrotechn. et Énerg., **53**, *1*, pp. 23–29 (2008).

6. G. De Pasquale *et al.*, *Performances improvement of MEMS sensors and energy scavengers by diamagnetic levitation*, International Conference on Electromagnetics in Advanced Applications (ICEAA), Torino, Italy, pp. 465–468, 2009.

7. D. Garmire *et al.*, *Diamagnetically Levitated MEMS Accelerometers*, Solid-State Sensors, Actuators and Microsystems Conference 2007, Transducers 2007, pp. 1203–1206, 2007.

8. W. Liu *et al.*, *Variable-capacitance micromotor with levitated diamagnetic rotor*, Electronic Letters, **44**, pp. 681–683 (2008).

9. F. Barrot, *Acceleration and inclination sensors based on magnetic levitation. Application in the particular case of structural health monitoring in civil engineering*, Ph.D. Thesis, EPFL, Laussane, 2008.

10. S. Palagummi, F.G. Yuan, *An efficient low frequency horizontal diamagnetic levitation mechanism based vibration energy harvester*, Proc. SPIE 9799, Active and Passive Smart Structures and Integrated Systems, March 2016.

11. G. Küstler, I.V. Nemoianu, *Theoretical and experimental evaluation on a counterintuitive diamagnetically stabilized levitation setup with permanent magnets*, 8th International Symposium on Advanced Topics in Electrical Engineering (ATEE), May 2013.

12. E. Cazacu, I.V. Nemoianu, *A novel configuration for static permanent magnet levitation*, Rev. Roum. Sci. Techn. – Électrotechn. et Énerg., **55**, *2*, pp. 153–160 (2010).

13. J. Ho, W.C. Wang, *An exploration about possibly levitating magnets using nonvertical configurations*, Progress In Electromagnetics Research Symposium, Japan, Tokyo August 2–5, 2006.

14. I.V. Nemoianu, G. Küstler, E. Cazacu, *Study of diamagnetically stabilized non-vertical levitation using the magnetic charge equivalence*, Int. J. Appl. Electrom., **38**, *2–3*, pp. 101–115 (2012).

15. M.D. Simon, L.O. Heflinger, A.K. Geim, *Diamagnetically stabilized magnet levitation*, Am. J. Phys., **69**, *6*, pp. 702–713 (2001).

16. P.C. Andrei *et al.*, *An efficient procedure to assess the static magnetization relationship*, Rev. Roum. Sci. Techn.–Électrotechn. et Énerg., **61**, *2*, pp. 101–105 (2016).

17. I.R. Ciric *et al.*, *A novel approach to the analysis of nonlinear magnetic fields produced by coils with imposed voltages*, Rev. Roum. Sci. Techn.–Électrotechn. et Énerg., **61**, *3*, pp. 213–216 (2016).